

1

2

Geophysical Research Letters

3

Supporting Information for

4

**Continental Scale Assessment of Variation in Floodplain Roughness with
Vegetation and Flow Characteristics**

5

6

Gabriel Barinas^{1,2}, Stephen P. Good^{1,2}, and Desiree Tullos^{1,2}

7

¹Water Resources Graduate Program, Oregon State University

8

²Department of Biological & Ecological Engineering, Oregon State University

9

10

Contents of this file

11

12

Extended methodology S1

13

Figures S1 and S2

14

Table S1

15

Dataset file description S1

16

Script files description S1

17

18

Additional Supporting Information (Files uploaded separately at Barinas et al., 2023)

19

20

21

Dataset file *fp_mannings.csv*

22

Script files *dataset.py* and *figures.py*

23

Required files: *NHDFlowline.csv*, *measurements.csv*, *gedi_L3L4.csv*, *ModisLC*,

24

geosfm.csv and *kalyanapu.csv*.

25 Extended Methodology S1

26 1. Floodplain roughness definition

27 Manning's equation (Manning, 1891) is extensively applied in hydraulic modeling and is
28 written as:

$$29 \quad Q = \frac{k}{n} S^{1/2} R^{2/3} A, \quad (S1)$$

30 where Q is discharge [$L^3 t^{-1}$], S is the friction slope, defining the energy loss along a
31 reach [$L L^{-1}$], R the hydraulic radius [L], A is cross-sectional area [L^2], k is a unit
32 conversion factor, and n is Manning's roughness coefficient. The coefficient n is a
33 representation of the roughness of the surface over which water is flowing and
34 incorporates surface characteristics such as smoothness, grain size, vegetation and/or
35 obstructions (Chow, 1959).

36 Here we conceptualize the floodplain as a wide, rectangular, cross-sectional area (see
37 Figure S1) and apply Manning's equation explicitly to the floodplain alone, separate from
38 the main river channel. The floodplain discharge, Q_{fp} , is isolated by taking the total
39 measured discharge, Q_t , and subtracting the discharge within the main channel, Q_{mc} . The
40 width of water in the floodplain, $w_{fp} = w_t - w_{mc}$, is assumed to be much greater than flow
41 depth, z_{fp} , and therefore the hydraulic radius of flow in the floodplain is approximately
42 equal to the floodplain flow depth (Reclamation, 2001). Rearranging Manning's equation
43 (eq. S1) for the floodplain and solving for floodplain roughness, n_{fp} , yields the following
44 relationship:

$$45 \quad n_{fp} = \frac{k w_{fp} z_{fp}^{5/3} S^{1/2}}{Q_t - Q_{mc}} \quad (S2)$$

46 2. Bankfull width estimation

47 Parameters corresponding to the total flow (Q_t , w_t) are collected during overbank
48 discharge measurements made by the United States Geological Survey (USGS) at
49 gauging stations. These total parameters were used to derive floodplain specific
50 parameters necessary to solve for the floodplain roughness. At bankfull depth, z_{bf} , the
51 width of the main channel, w_{mc} , is not specified or measured, and must be estimated by
52 determining the cross-sectional geometry of the main channel and floodplain. A
53 piecewise function based on measurements of w and z was used to determine w_{mc} , with
54 the main channel depth assumed a power function of the width, i.e. $z \propto w$ (Durand et al.,
55 2016), and the floodplain as sloping linearly away from bankfull stage. The piecewise
56 form of w as a function of z was then expressed as:

$$57 \quad w = \frac{(z - z_0)^{1/s}}{u} \quad \text{when } z < z_{bf} \quad (S3a)$$

58
$$w = m(z - z_{bf}) + \frac{(z_{bf} - z_0)^{1/s}}{u}, \quad \text{when } z \geq z_{bf} \quad (\text{S3b})$$

59 where m is the cross-sectional up-slope of the floodplain, u and s are parameters that
60 define the shape of the main channel curvature, and z_0 defines its starting point.

61 Discharge in the main channel above flood stage was represented as a rectangular cross-
62 section, as such flow in the main channel Q_{mc} should assumed to be proportional to
63 $(z)^{5/3}$, following Manning's function (eq S1). When the flow reaches bankfull condition
64 i.e. $z = z_{bf}$, $Q_{mc} = Q_{bf}$, and thus the constant of proportionality is equal to $Q_{bf}/z_{bf}^{5/3}$,
65 and Manning's function (eq. S1) for the main channel flow above bankfull was simplified
66 as:

67
$$Q_{mc} = \left(\frac{Q_{bf}}{z_{bf}^{5/3}} \right) z^{5/3} \quad (\text{S4})$$

68 where Q_{bf} is the flow at flood stage given that $Q_{mc} = Q_t$ when $z = z_{bf}$.

69 **3. Data sources and quality control**

70 Most of the parameters (Q_t, w_t, z) required for the calculation of Manning's n with Eq.
71 S2-S4, were obtained from the field measurements datasets available from the USGS
72 WaterData platform (USGS, 2021a). The WaterData platform is part of the USGS efforts
73 to monitor, assess, and deliver information about streamflow quality, use and availability.
74 The platform provides access to field measurements at nearly 73,000 sites under USGS
75 management. Consistent with Slater et al., (2015), the flood stage height (z_{bf}) was
76 obtained from the WaterWatch platform (NWS, 2021). These values were determined by
77 the National Weather Service by defining the flood stage as the lowest bank at which
78 inundation of the surrounding area begins to cause damage. Friction slope estimates
79 were obtained from the National Hydrography Dataset (USGS, 2021b), a database of
80 features that includes a drainage network of US waterbodies.

81 Quality control measures on the floodplain data involved multiple steps. The rating
82 curves at USGS sites are regularly adjusted to adapt the relationship to geometry
83 changes associated with erosion or deposition at a gauging location. To account for this
84 effect, only river discharge and geometry measurements where the measured values
85 were within 10% of the respective rating curve value were included in the analysis.
86 Additionally, sites with a low number of measurements over the flood stage (< 3) were
87 also removed. As a way of avoiding the calculation of n with measurements with a high
88 level of uncertainty in the width-depth relationship (eq. 3), as evidenced by regression
89 curves with a high root mean squared error (RMSE), only samples with width
90 measurements higher than 1.96 times the RMSE of the fit in eq. 3 were considered (Liu,
91 2011). Furthermore, a large percentage of sites from the resulting dataset (27%) had a
92 slope set at a value of 0.0001 within the National Hydrography Dataset, representing a

93 minimum fixed value within the database. Due to the high uncertainty and potential
94 error from including the fixed minimum slopes, these 298 sites were also excluded from
95 analysis.

96 In addition, the results of this work are subject to limitations of the USGS gaging network
97 and to uncertainties inherent in gaging stochastic and modified systems. The lack of
98 representation of certain geographic areas within the USGS gaging network have been
99 reported elsewhere (Kiang et al., 2013), as have some of the drivers of temporal noise
100 and uncertainty in streamflow over time (Tu et al., 2023). Application of the results
101 outside the geographic areas and LULC (Land Use Land Cover) conditions from which
102 these data were derived may generate uncertainties that we were unable to quantify with
103 this analysis.

104 **4. Remote sensed vegetation datasets**

105 Flow in floodplains is expected to be strongly influenced by the vegetation in the
106 floodplain (Box et al., 2021) but vegetation characteristics (density, height, etc.) are not
107 typically measured in the field during flood conditions. Here we used aboveground
108 biomass density, B [$M L^{-2}$], and vegetation canopy height, h_{veg} , as characterized by the
109 NASA Global Ecosystem Dynamics Investigation (GEDI). GEDI utilizes a full waveform
110 Light Detection and Ranging (LiDAR) system to make measurements of vegetation
111 structure at 25m resolution (Potapov et al., 2021), which are then aggregated to a 1km
112 spatial resolution grid. In this work, for each USGS site, we obtained the canopy height
113 estimates from the L3B version 2 gridded product (Dubayah et al., 2021) and the
114 aboveground biomass estimates from the L4B version 2 gridded product (Dubayah et al.,
115 2022).

116 Within GEDI's L4B dataset, there is a Prediction Stratum (PS) classification, determined by
117 plant functional types described as: Deciduous Broadleaf Trees, Evergreen Broadleaf
118 Trees, Evergreen Needleleaf Trees, Deciduous Needleleaf Trees, and Grasses, Shrubs, and
119 Woodlands grouped as one class. This classification was used to categorize our dataset
120 based on the level of biomass and canopy height by extracting the GEDI data from the
121 pixel where each gauge location fell within (See Table S1). It is important to note that
122 Gridded GEDI datasets, while providing unique information about vegetation height and
123 biomass, is limited by its 1km resolution, capable of measuring only vegetation above a
124 certain height.

125 **5. Theoretical modeling**

126 Prior research suggests that n is proportional to the square-root of the vegetation
127 inundation fraction, i.e. $n \propto (z_{fp}/h_{veg})^{1/2}$, and that it is also related to flow velocity and
128 vegetation properties (Kouwen & Fathi-Moghadam, 2000). A mathematical model by

129 Kouwen was based on data from four tree species:

130
$$n = 0.228 \left(\frac{V}{\sqrt{\frac{\xi E}{\rho}}} \right)^{-0.23} \left(\frac{yn}{h} \right)^{0.5} \quad (\text{eq. 5})$$

131 where V is flow velocity, ξE is a vegetation index, ρ is the density of the fluid, and yn/h is
132 the depth of submergence (z_{fp}/h_{veg}), and 0.228 and -0.23 empirically fit. Based on this
133 approach, we formulate an analogous expression incorporating GEDI derived vegetation
134 properties as $c = a_1 V^{a_2} B^{-a_3}$, where a_1 , a_2 and a_3 are model parameters, B is
135 aboveground biomass, V is flow velocity, and c is Manning's n normalized by the square
136 root of vegetation inundation fraction, i.e. $c = n/(z_{fp}/h_{veg})^{1/2}$. To ensure positive c (and
137 n) values, the linearized equation:

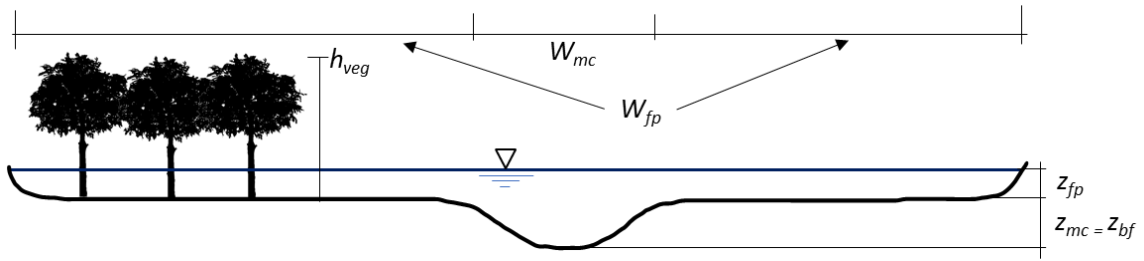
138
$$\ln(c) = a_1 + a_2 \ln(V) + a_3 \ln(B) \quad (\text{eq. 6})$$

139 was fit to values of c , V , and B at USGS sites in our dataset to determine a_1 , a_2 and a_3 .

140 To limit the uncertainty caused by outliers in the dataset during the development of the
141 model, the range of c values was restricted with the use of the interquartile range (IQR)
142 (Vinutha et al., 2018). The minimum c value included in the analysis was the first quartile
143 minus 1.5 times the IQR and the maximum value was the third quartile plus 1.5 times the
144 IQR, where the IQR is equal to the difference between the third and the first quartile.

145 The developed function underwent cross-validation by splitting the USGS dataset, after
146 quality control, into five randomized equal subsets, with each subset serving as
147 validation during separate simulations. Subsequently, we combined all five validation
148 subsets to create a comprehensive validation dataset that includes all of the original
149 USGS gauge locations. This approach enables us to thoroughly assess the applicability
150 and representativeness of our empirical function across the entire set of gauge locations.
151 This new validation set was then used to compare the performance of our model against
152 other works.

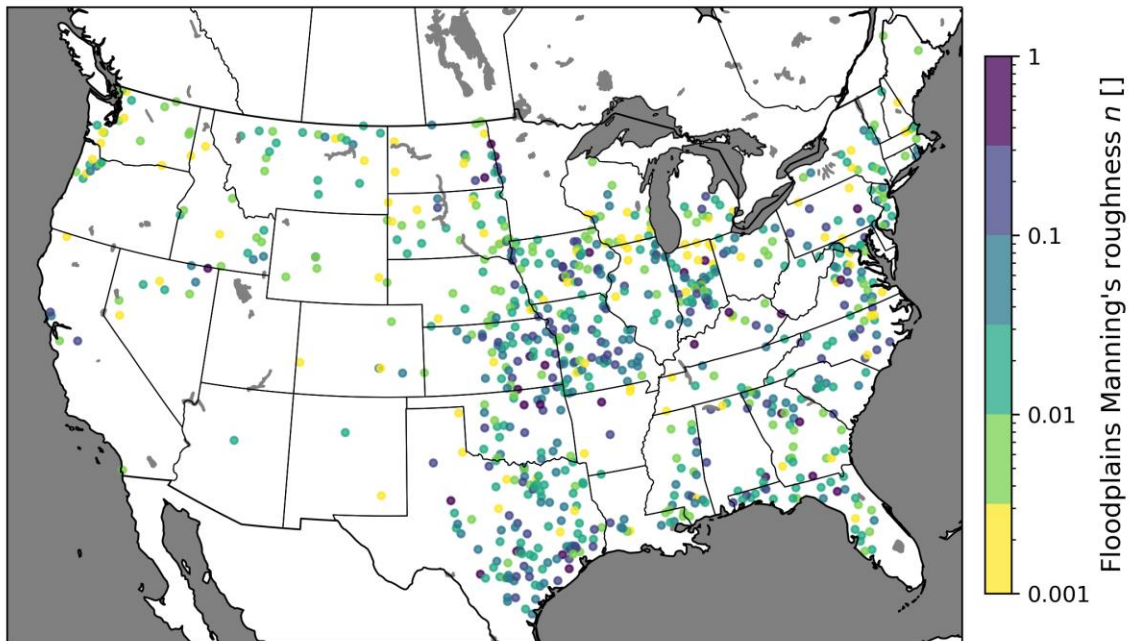
153 **Figures S1 and S2**



154

155 **Figure S1** – Cross section diagram showing the variables used in the analysis. W_{mc} is the
156 width of the main channel, W_{fp} is the width of the floodplain, Z_{mc} and Z_{bf} are the depth of
157 the main channel during bankfull conditions, and h_{veg} is the height of the vegetation.

158



159

160 **Figure S2** - Floodplain roughness (Manning's n) estimates for USGS sites.

161 **Table S1**

162 Mean floodplain Manning’s *n* and Aboveground Biomass (*B*) [Mg/Ha] classified by tree
 163 structure and ranges of vegetation height. Values given are the median ± one median
 164 absolute deviation and the (samples count). The median vegetation height for these sites
 165 was 10m, while the 33rd and 66th percentiles were 7.4m and 13.5m. Values of 7.5m and
 166 14m for vegetation height were selected for the ranges in order to have roughly the
 167 same number of total samples in each range.

Land Cover	Floodplain Vegetation Biomass, <i>B</i> [Mg/Ha], floodplain <i>n</i> , and (sample count)							
	<i>h_{Veg}</i> <7.5m		<i>h_{Veg}</i> 7.5-14m		<i>h_{Veg}</i> >14m		All heights	
	<i>B</i>	<i>n</i>	<i>B</i>	<i>n</i>	<i>B</i>	<i>n</i>	<i>B</i>	<i>n</i>
Deciduous Broadleaf Trees	25 ±6 (340)	0.023 ±0.022	63 ±20 (518)	0.026 ±0.022	130 ±29 (652)	0.026 ±0.020	77 ±45 (1514)	0.025 ±0.022
Evergreen Broadleaf Trees	37 ±0 (5)	0.005 ±0.004	50 ±0 (15)	0.025 ±0.022	98 ±28 (150)	0.032 ±0.022	95 ±25 (170)	0.030 ±0.022
Evergreen Needleleaf Trees	62 ±32 (10)	0.007 ±0.006	44 ±5 (37)	0.011 ±0.009	108 ±2 (79)	0.011 ±0.009	106 ±19 (126)	0.010 ±0.008
Grasses, Shrubs and Woodlands	12 ±8 (976)	0.012 ±0.010	28 ±16 (540)	0.038 ±0.034	51 ±2 (196)	0.022 ±0.013	18 ±12 (1737)	0.017 ±0.014
Unclassified	6 ±2 (141)	0.021 ±0.017	44 ±15 (264)	0.025 ±0.021	106 ±36 (279)	0.020 ±0.016	44 ±36 (787)	0.023 ±0.018
All GEDI land cover classes	15 ±10 (1472)	0.014 ±0.012	44 ±20 (1374)	0.028 ±0.024	110 ±38 (1356)	0.023 ±0.017	38 ±27 (4927)	0.021 ±0.018

168

169 **Dataset**

170 The dataset included as part of the Supplementary Information document is the result of
171 the analysis that took place during this study. The dataset file named '*fp_mannings.csv*',
172 consists of 4,927 calculations of Manning's n at each of the 804 USGS gauge sites that
173 remained after quality control. The file also includes all variables collected and derived
174 from USGS field measurements: discharge, width, depth (total, main channel, and
175 floodplain), channel slope, site ID, coordinates, and number of estimates on that site.

176 **Scripts**

177 Included as supplementary information there are two scripts: *dataset.py* and *figures.py*.

178 The *dataset.py* script automates the process of calculating the Manning's n
179 *fp_mannings.csv* file. It is divided into 3 sections: a SETUP section for module and file
180 imports, a RUN section for defining the main function and running it for each state, and
181 a MERGE section that puts together the results of each state into a single file. This script
182 requires the *NHDFlowline.csv* and *measurements.csv* files which are included in Barinas et
183 al., (2023). Other necessary files are downloaded automatically from USGS websites for
184 each site: <https://nwis.waterdata.usgs.gov/> for site coordinates;
185 <https://waterdata.usgs.gov/> for rating curves; and <https://waterwatch.usgs.gov/> for flood
186 stages.

187 The *figures.py* script creates the figures included in the main paper and in this document.
188 This script is divided into 4 sections: IMPORTS loads the necessary modules and files
189 required; MAP corresponds to Figure S2 in this document; MODEL corresponds to Figure
190 2 in the main manuscript; HEATMAP corresponds to figure 1 in the main manuscript, and
191 VALIDATION corresponds to figure 3 in the main manuscript. This script requires remote
192 sensed data by the Ecosystem Dynamics Investigation Mission GEDI. All GEDI data
193 included in the *gedi_L3L4.csv* file refers to the pixel value where all USGS sites in the
194 *fp_mannings.csv* file fell within and the data collected corresponds to the L3 and L4B
195 version 2 gridded products (Dubayah et al., 2022). Finally, for the validation section of
196 the script, the file *ModisLC.csv*, which contains the MODIS land cover classification
197 corresponding to each gauge location, and the files *geosfm.csv* and *kalyanapu.csv*, which
198 contains the values of n for each land cover type as presented in the original papers
199 (Asante et al., 2008; Kalyanapu et al., 2009).

200